

Thermal Fatigue Under Multiaxial Stresses

Feng Junyi, Dang Zijiu, Bian Menxin
University of Science and Technology, Beijing, China

(Third International Conference on Biaxial/Multiaxial
Fatigue, April 3-6, 1989, Stuttgart, FRG)

Abstract

In this article, thermal fatigue problem under multiaxial (plane) stresses has been investigated with quantitative analysis and tests.

The circular cylinder specimens were tested under thermal fatigue which was in step with mechanical fatigue.

The axial force F_x only induced the axial stress σ_x , strain ϵ_x , and the plastic strain ϵ_{px} . All the temperature cycles were same, so we had different ratios σ_x/σ_0 , ϵ_x/ϵ_0 , $\epsilon_{px}/\epsilon_{p0}$ with different axial forces. In the result, straight thermal fatigue cracks in different directions and checks in different states occurred on surfaces of the specimens.

The transient temperature, stress and strain fields have been calculated by the thermal elasto-plastic Finite Element Method (FEM).

Compared the test results with that of calculation, we've come to the conclusion that the state of thermal fatigue cracks is dependent on the stress state and the plastic strain state, not on the strain state. The direction of cracks is perpendicular to the greater main stress and the greater plastic strain. Thermal fatigue checks will occur when one main stress is about the same as the other one and one plastic strain is about equal to another.

Key words: thermal fatigue, multiaxial stress

Thermal Fatigue Under Multiaxial Stresses

Feng Junyi, Dang Zijiu, Bian Mengxin
University of Science and Technology, Beijing, China

(Third International Conference on Biaxial/Multi-axial
Fatigue, April 3-6, 1989, Stuttgart, FRG)

1. Introduction

Thermal fatigue often occurs in engineering. After many times of heating and cooling, thermal fatigue cracks are created on the surfaces of components, such as dies, rollers and so on. Some cracks may be big enough to make the components lose their load capacity and bring about a great loss in economy. So, investigating thermal fatigue problems has a great value not only in theoretical but also in economic aspects.

Thermal fatigue problems are very complex, they involve many factors, such as transient temperature, transient stresses, environments and the property changes of materials with temperature. So research is basically concentrated on to qualitative analysis and test simulations.

Coffin's formula $\Delta \epsilon_p N_f^c = c$ laid the foundation of quantitative analysis of thermal-mechanical fatigue. We can calculate the thermal fatigue life N_f with the cyclic plastic strain range $\Delta \epsilon_p$. Because the thermal fatigue is a transient problem and involves many factors, so there are many difficulties in quantitative analysis works. The quantitative analysis of thermal fatigue under multiaxial stresses, as considering the propagation patterns and states of cracks under different stress states, is important in thermal fatigue designs, but little work has been done up to now.

In this article, the thermal fatigue problem of 3Cr2W8V steel under biaxial stresses has been investigated with quantitative analysis and tests.

2. Thermal Fatigue Test

1. The test purpose

The tests were carried out to obtain different stress states, regularities of propagation and different states of thermal fatigue cracks, so as to illustrate the effects of the stress states on the thermal fatigue. The surfaces of specimens are under biaxial stresses, therefore, only by altering the ratios of the main stresses or changing the torsional stresses, the states of stresses could be changed.

2. The test method

We selected the circular cylinder specimens of 3Cr2W8V steel, shown in Fig.1, in order to regulate the stress states easily. The temperature and the axial force had been cycling in step with each other, the force maintained zero during the slow heating, but it was exerted when cooling. The cyclic curves are

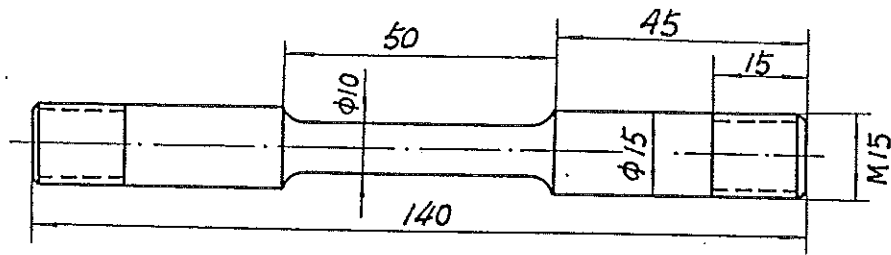


Fig.1 The thermal fatigue specimen

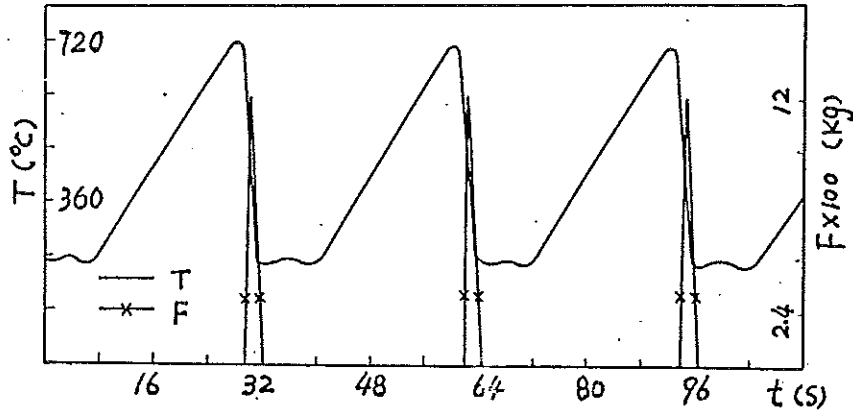


Fig.2 The cyclic curves of temperature and axial force corresponding to the time

shown in Fig.2. The maximum axial force F_{xmax} could be adjusted, so the axial stress σ_x , axial strain ϵ_x and the axial plastic strain ϵ_{px} could be adjusted as well. All the specimens had borne the same temperature cycles, so the circumferential stress σ_θ , circumferential strain ϵ_θ and the circumferential plastic strain $\epsilon_{p\theta}$, which were induced by the temperature gradients in the specimens, were same in all specimens.

Hence we had different ratios σ_x / σ_θ , $\epsilon_x / \epsilon_\theta$ and $\epsilon_{px} / \epsilon_{p\theta}$ with different forces, or we had different stress states. Then we studied the thermal fatigue problem under these stress states.

In the tests, $T_{max}=720^\circ\text{C}$, $T_{min}=210^\circ\text{C}$. The number of cycles was 150 for every specimen. The transformation temperature A_{c3} of the 3Cr2W8V steel is 850°C , so there was no phase transformation in the thermal fatigue cycles.

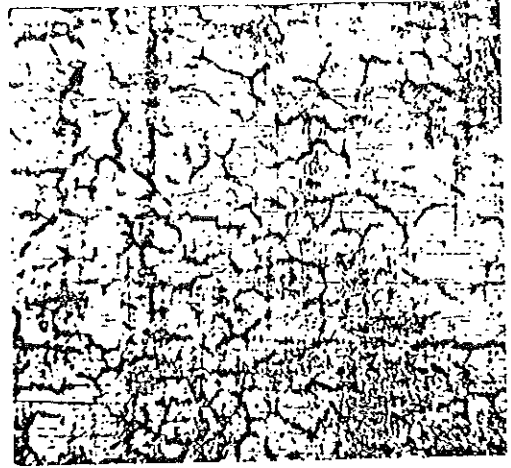
Because of the slow heating and the force maintained zero, there were no stresses in the specimens during heating. When quenching, the temperature rate was very high, so the temperature gradients were great in the specimens. With self-constraint of the specimens, the circumferential stress σ_θ , strain ϵ_θ and $\epsilon_{p\theta}$ occurred, and also the mechanical stress σ_x , strain ϵ_x and ϵ_{px} occurred as the axial force F_x was exerted at the same time. Hence we had a biaxial stress state on the surface of a specimen when quenching.

3. The test equipment

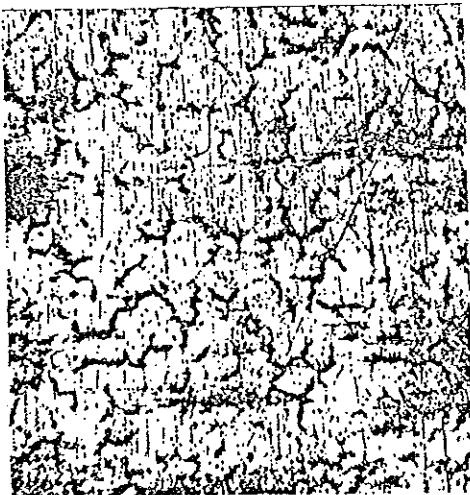
The tests were carried out on the Gleeble--1500 machine produced by the Duffers Scientific, INC of USA. This machine is controlled by a computer, so it is easy to operate. It can gather data and plot figures automatically. The temperature, mechanical load and the water-spraying system can be programmed



(a) $F_x=0$



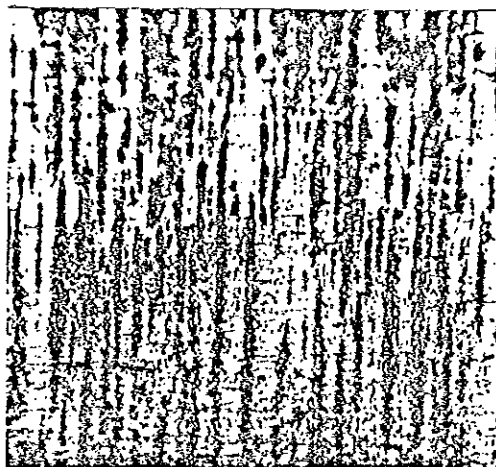
(b) $F_{xmax}=600$ kg



(c) $F_{xmax}=1200$ kg



(d) $F_{xmax}=1800$ kg



(e) $F_{xmax}=2400$ kg

Fig.3 Micrographs of the thermal fatigue cracks, 150cycles, x100 (the horizontal line is the axis of specimen)

in step with each other. So the results of the tests are reliable. The clamping and water-spraying apparatus were specially designed by the authors.

4. The test results

The quenching T-t curve is shown in Fig.4. Micrographs of the thermal fatigue cracks propagated on surfaces of the specimens after 150 cycles are shown in Fig.3.

From Fig.3, we can see the following characters of the cracks. As Fig.3(a) shown, straight cracks occurred corresponding to the zero force, and they are parallel to the axis of the specimen. The great force induced also the straight cracks, but these cracks are perpendicular to the axis of the specimens, shown as Fig.3(e). There are only thermal fatigue checks on the surface of the specimen which bore a moderate axial force, as Fig.3(c) shown. With the small forces we had the rectangular checks which are parallel to the specimen's axis, as Fig.3(b) shown. A moderate great force induced also rectangular checks which are perpendicular to the axis, as Fig.3(d).

Therefore, the directions and states of the thermal fatigue cracks changed with the force's changing.

3. Numerical Calculation of The Transient Temperature Field

The stresses and strains in thermal stress fatigue problems are dependent on the transient temperature field of specimens or components. But the transient temperature fields are very difficult to be determined as to some properties of materials vary with temperature. That is why up to now the quantitative analyses of the thermal stress fatigue problems have not been done. The authors have calculated the transient temperature with numerical method in this artical. The following is the synopsis of the theory and the method.

The differential heat conduction equation for the axisymmetrical problem without heat sources is

$$\frac{\partial T}{\partial t} = \frac{k}{\rho C_p} \left(\frac{\partial^2 T}{\partial r^2} + \frac{1}{r} \frac{\partial T}{\partial r} + \frac{\partial^2 T}{\partial x^2} \right) \text{-----(1)}$$

The second boundary condition is

$$-k \frac{\partial T}{\partial n} \Big|_{\Gamma} = q \text{-----(2)}$$

The third boundary condition is

$$-k \frac{\partial T}{\partial n} \Big|_{\Gamma} = \alpha (T - T_f) \Big|_{\Gamma} \text{-----(3)}$$

Here k is heat conduction coefficient, Cp is specific heat, q is heat-flow density on the second boundary and α the heat-exchange coefficient on the third boundary, they are all functions of temperature T.

From the above equations we have induced the following equation of the Finite Element Method

$$[K]\{T\} + [N]\left\{\frac{\partial T}{\partial t}\right\} = \{P\} \text{-----(4)}$$

The backward finite difference is substituted for the derivative of temperature with respect to time, we have the recurrence formula

$$([K] + \frac{[N]}{\Delta t})(T)_t = (P)_t + \frac{[N]}{\Delta t}(T)_{t-\Delta t} \quad \text{-----(5)}$$

with the initial condition:

$$T|_{t=0} = T_0. \quad \text{-----(6)}$$

We can obtain the numerical solution of the temperature field step by step as the time goes on.

The key to the question is how to determine the heat-flow density q and the heat-exchange coefficient α in heat conduction. The authors determined them by comparing the temperatures calculated by the Finite Element Method with that measured on the surfaces of specimens, and by repeating calculations. Finally, we obtained the numerical solution of the temperature fields in the specimens. Fig.4 and Fig.5 are the temperatures we calculated and measured on the specimen's surface. From the figures we can see that the two curves tally with each other, so the results of our calculation are reliable.

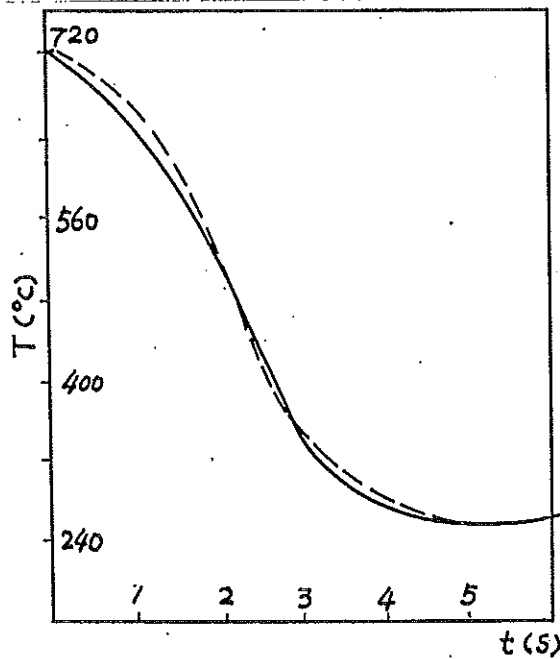


Fig.4 The quenching T-t curve

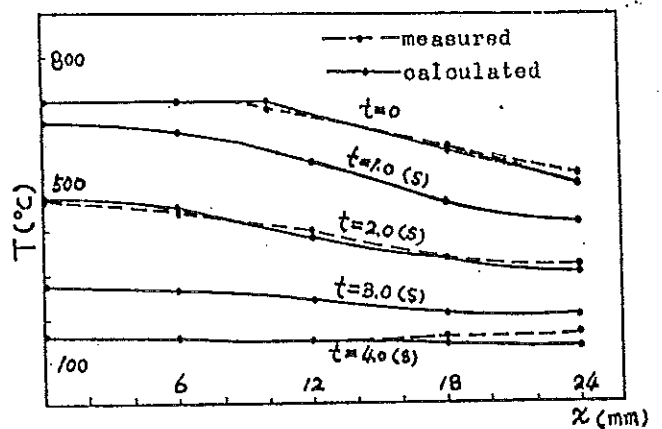


Fig.5 The temperature distribution along the axis of specimen ($x=0$ is the symmetrical cross section of the specimen)

4. Numerical Calculation of The Transient Stresses and Strains

From the results of the transient temperature field calculated above, we can calculate the stresses and strains of specimens by the thermal elasto-plastic Finite Element Method (FEM). The mechanical properties of the material change while quenching, so we tested the material on the MTS machine from 20°C to 720°C, and obtained the stress-strain relations at different temperatures.

The basic equation of the FEM is

$$[K]_{i-1} \Delta(\sigma)_i = \Delta(P)_i \quad \text{----- (7)}$$

From the equation we can calculate the stresses and strains. Here $[K]_{i-1}$ is the rigid matrix before the time increment Δt_i , $\Delta(P)_i$ and $\Delta(\sigma)_i$ are the increments of loads and displacements in Δt_i . Then the stress increments $\Delta(\sigma)_i$ can be calculated with $\Delta(\sigma)_i$.

The time increments Δt_i and the finite elements are all the same to that used in the temperature's calculation.

The stresses σ_x, σ_θ , strains $\epsilon_x, \epsilon_\theta$ and the plastic strains $\epsilon_{px}, \epsilon_{p\theta}$ in a specimen calculated with the above method are shown in Fig.6 and Fig.7.

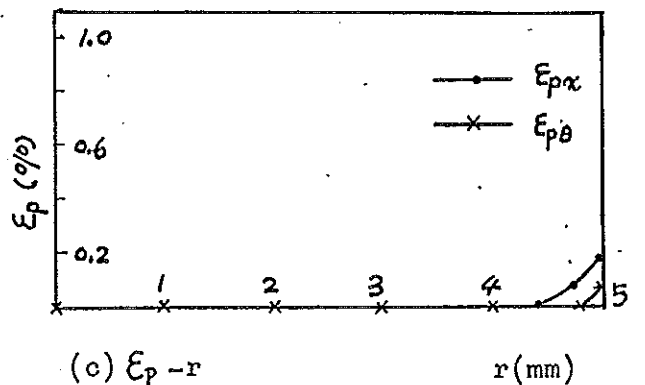
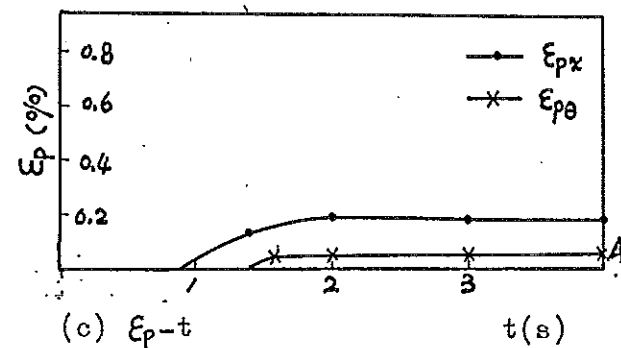
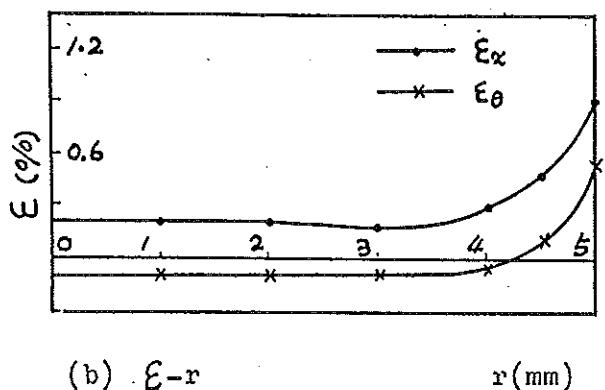
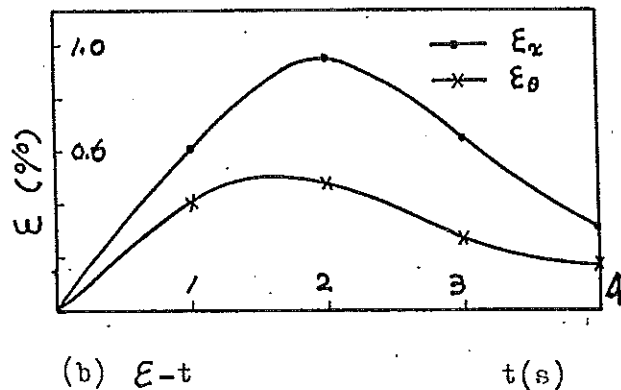
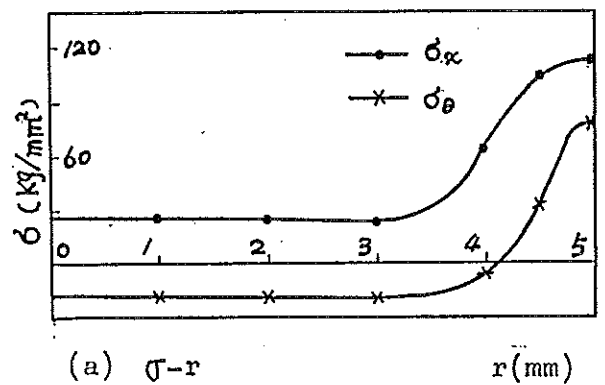
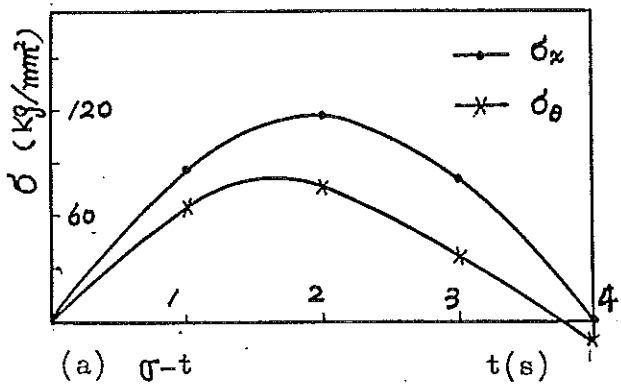


Fig.6 The curves of stresses, strains and plastic strains corresponding to the time
($r=5.0\text{mm}$, $x=3.0\text{mm}$)
 $F_{x\text{max}}=2000\text{ kg}$

Fig.7 The stress, strain and the plastic strain distributions along the radial
($t=1.50\text{s}$, $x=3.0\text{mm}$)
 $F_{x\text{max}}=2000\text{ kg}$

In Fig.7, the maximum stresses in the region near the boundary ($r=5.0\text{mm}$) exceeded the elastic limit of the material, but there is still an elastic region near the axis of the specimen.

5. Analysis and Discussion

Curves of the maximum stresses, strains and plastic strains on surfaces of the specimens corresponding to the maximum axial forces have been drawn in Fig.8. Fig.9 shows the relations between states of cracks and that of stresses and strains.

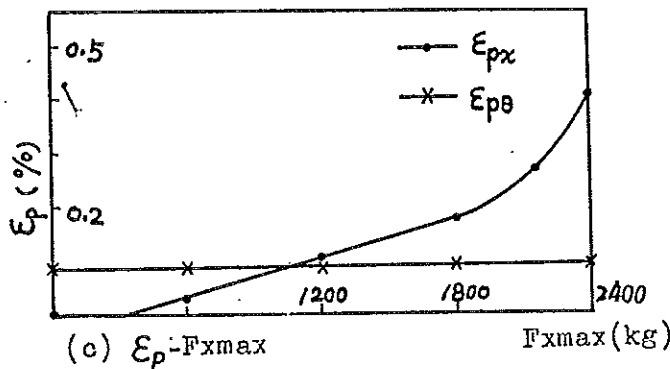
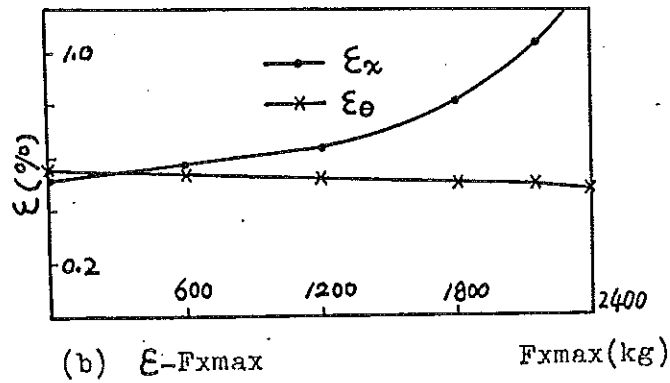
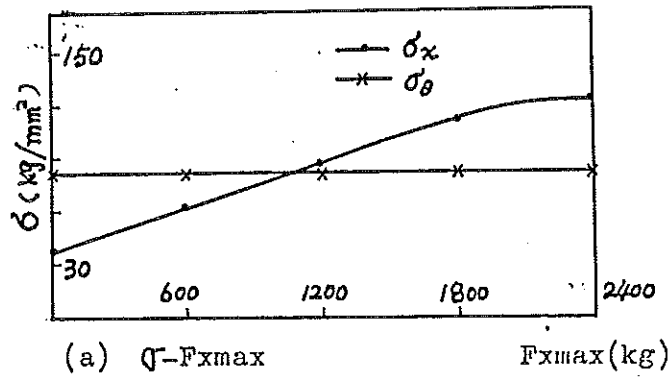


Fig.8 The curves of stresses, strains and plastic strains corresponding to the axial force
($t=1.50\text{s}$, $r=5.0\text{mm}$, $x=3.0\text{mm}$)

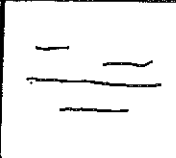

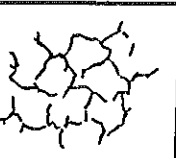


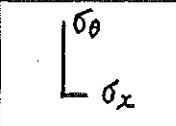

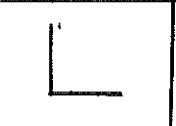


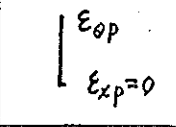


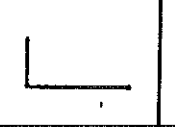

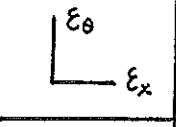

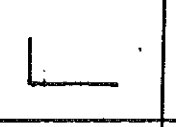
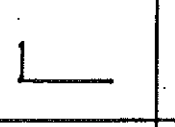

states of cracks					
	axial cracks	axial rectangular checks	checks	circumferential rectangular checks	circumferential cracks
states of stresses					
	$2\sigma_x \leq \sigma_\theta$	$1.4\sigma_x \approx \sigma_\theta$	$\sigma_x \approx \sigma_\theta$	$\sigma_x \approx 1.4\sigma_\theta$	$\sigma_x \geq 1.5\sigma_\theta$
states of plastic strains					
	$\epsilon_{xp} \ll \epsilon_{\theta p}$	$2.2\epsilon_{xp} \approx \epsilon_{\theta p}$	$\epsilon_{xp} \approx \epsilon_{\theta p}$	$\epsilon_{xp} \approx 2.3\epsilon_{\theta p}$	$\epsilon_{xp} \gg 4\epsilon_{\theta p}$
states of strains					
	$\epsilon_x \approx \epsilon_\theta$		$\epsilon_x > \epsilon_\theta$		$\epsilon_x \gg \epsilon_\theta$
F_{xmax}	0	600	1200	1800	2400(kg)

Fig.9 The sketch map of the relations between the states of thermal fatigue cracks and that of stresses, strains and plastic strains

The figures show that the circumferential stress σ_θ is two or more times as great as the axial stress σ_x , and the circumferential plastic strain $\epsilon_{\theta p}$ is far greater than the axial plastic strain ϵ_{xp} , that is $\sigma_\theta > 2\sigma_x$ and $\epsilon_{\theta p} \gg \epsilon_{xp}$, on the specimen's surface when the axial force F_{xmax} equals zero. The corresponding cracks are in straight lines and they are parallel to the axis, or perpendicular to σ_θ and $\epsilon_{\theta p}$. When F_{xmax} takes a moderate value (about 1200kg), σ_θ is about equal to σ_x and $\epsilon_{\theta p}$ to ϵ_{xp} , or $\sigma_\theta \approx \sigma_x$ and $\epsilon_{\theta p} \approx \epsilon_{xp}$, then checks appear. The great force makes $\sigma_x > 1.5\sigma_\theta$ and $\epsilon_{xp} > 4\epsilon_{\theta p}$, and then straight cracks occur also, but they are perpendicular to the axis, or to σ_x and ϵ_{xp} .

Although the axial force F_{xmax} changed in a large range, the direction of the maximum strain didn't alter, that is $\epsilon_x > \epsilon_\theta$ in all the above cases.

From the above analysis, we've come to the following conclusions. The states of thermal fatigue cracks can be changed with the changing of the states of stresses and plastic strains, which can be induced by the increase of the axial force. The straight cracks are always perpendicular to the maximum stress σ_1 and the maximum plastic strain ϵ_{p1} . Checks occur when two main stresses are about the same, and also two plastic strains are about the same.

E. Conclusions

(1). The states of thermal fatigue cracks are dependent on that of stresses and plastic strains, not on that of strains.

(2). Under the states of $\sigma_1 > 1.5 \cdot \sigma_2$ and $\epsilon_{p1} > 3 \cdot \epsilon_{p2}$, the thermal fatigue cracks will be in straight lines, and perpendicular to σ_1 and ϵ_{p1} .

(3). When two main stresses are about the same and also two plastic strains are about the same, thermal fatigue checks will occur.

(4). Stress state must be considered in thermal fatigue designs and tests, because thermal fatigue cracks have something to do with the states of stresses and plastic strains.

Our conclusions are applicable for the famous Coffin's test. The specimen was a thin wall circular cylinder which was constrained rigidly at its two ends. The temperature field was uniform in the specimen. Because it was free in radial and circumferential directions, therefore we have the states

$$\sigma_\theta = \sigma_r = 0, \quad \epsilon_\theta = \epsilon_r = \beta \cdot \Delta T, \quad \epsilon_{p\theta} = \epsilon_{pr} = 0, \quad \epsilon_x = \epsilon_x^T + \epsilon_{ex} + \epsilon_{px} = 0,$$

but $\sigma_x \neq 0$ and $\epsilon_{px} \neq 0$.

According to our conclusions, the cracks might be in straight lines, and they might be perpendicular to the maximum stress σ_x and the maximum plastic strain ϵ_{px} , or to the axis of the specimen. In fact, the cracks in Coffin's test did so.

Acknowledgement

We would like to thank Mr. Chen Weichang, Ms. Wu Na and Ms. Zhana Yan for their kind assistance in the thermal fatigue tests.

References

1. D.A. Spera, Thermal Fatigue of Materials and Components, ASTM, STP, 1976
2. Coffin, L.F., Jr. and Wesley, R.P., Transactions, ASME, vol.76, Aug., 1954
3. L.F. Coffin, Internal Stress and Fatigue in Metal, Pr. Symp. 1959
4. P. Stanley, F.S. Chau, The Effects of The Temperature-Dependence of Properties on The Thermal Stresses in Cylinders, 1977, University of Manchester.
5. Shuji Taira and Tatsuo Inoue, Thermal Fatigue Under Multi-axial Stresses, PIC, 1969, Sep.22nd-26th
6. D.J. Littler, Thermal Stresses and Thermal Fatigue, PIC, 1969, Sep.22nd-26th